New markers for murine memory B cells that define mutated and unmutated subsets

Shannon M. Anderson,[1] Mary M. Tomayko,[3] Anupama Ahuja,[2] Ann M. Haberman,[1] and Mark J. Shlomchik[1,2]

[1]Section of Immunobiology, [2]Department of Laboratory Medicine, and [3]Department of Dermatology, Yale University School of Medicine, New Haven, CT 06510

The study of murine memory B cells has been limited by small cell numbers and the lack of a definitive marker. We have addressed some of these difficulties with hapten–specific transgenic (Tg) mouse models that yield relatively large numbers of antigen–specific memory B cells upon immunization. Using these models, along with a 5–bromo-2'–deoxyuridine (BrdU) pulse–label strategy, we compared memory cells to their naive precursors in a comprehensive flow cytometric survey, thus revealing several new murine memory B cell markers. Most interestingly, memory cells were phenotypically heterogeneous. Particularly surprising was the finding of an unmutated memory B cell subset identified by the expression of CD80 and CD35. We confirmed these findings in an analogous V region knock–in mouse and/or in non–Tg mice. There also was anatomic heterogeneity, with BrdU+ memory cells residing not just in the marginal zone, as had been thought, but also in splenic follicles. These studies impact the current understanding of murine memory B cells by identifying new phenotypes and by challenging assumptions about the location and V region mutation status of memory cells. The apparent heterogeneity in the memory compartment implies either different origins and/or different functions, which we discuss.

Abbreviations used: Ab, antibody; AFC, antibody-forming cell; Ag, antigen; AP, alkaline phosphatase; APC, allophycocyanin; BCR, B cell receptor; CDR, complementarity-determining region; FW, framework region; GC, germinal center; MFI, mean fluorescence intensity; MZ, marginal zone; NIP, 4-hydroxy-3-nitroiodophenyl; NP, 4-hydroxy-3-nitrophenyl; Tg, transgenic.

Immunological memory is the defining feature of the adaptive immune system. Memory is an emergent property of the immune system that derives from a variety of mechanisms. The immune host has standing antibody (Ab) titers that block or modify reinfection. Recall responses are faster, larger, and qualitatively different than primary responses (1). Part of this effect is caused by increased precursor frequency of antigen (Ag)-specific T and B cells; these more numerous cells also do not respond the same way as naive cells (2–4). How memory cells differ from naive cells is thus of fundamental interest in understanding immunological memory.

There is surprisingly little known about memory B cells, with most information coming from human studies. Presumably because of the constant exposure to antigens, humans have an abundance of memory-like cells, as defined by the widely accepted marker CD27 (5–7). The use of CD27 as a memory marker has allowed flow analysis and the purification of memory B cells, enabling in vitro and gene expression studies (2, 4, 8–10). These studies have provided insight into intrinsic differences between naive and

memory B cells. For example, Tangye et al. have shown that memory B cells are more apt to proliferate and differentiate in vitro into Ab-forming cells (AFCs) under certain conditions of stimulation (4, 9). However, the origins and age of memory cells in humans, as well as their Ag specificity, are difficult to discern; additionally, the properties of human memory cells cannot be tested in vivo.

The murine system, on the other hand, has been hampered by small numbers of memory cells (∼5,000–50,000 Ag-specific cells per immune mouse spleen [11–13]), as well as a lack of generally agreed-upon markers for memory cells. Instead of specific memory markers, workers have used isotype switch in a cell that lacks germinal center (GC)–specific markers as a surrogate for memory identity (14, 15). However, the murine system enables genetic manipulation and cell transfer to test the roles of genes and cell subsets (16, 17). Further, the exact precursor–product relationship between naive and memory cells can be established. The age of memory cells can also be known, and such cells can be studied when the primary response has waned completely. Thus far, these potential advantages have largely been untapped.

The online version of this article contains supplemental material.

It would be ideal to have a murine memory system that generated larger numbers of cells. This would permit a better definition of memory cell surface markers and enable in vitro functional analysis. Surface markers can provide insight into memory B cell biology; for example, human memory B cells have elevated levels of the costimulatory molecules CD80 and CD86 compared with naive cells (18–20). In addition, surface marker expression could define biologically meaningful heterogeneity, as is the case for memory T cells (21). One limitation in efforts to define markers and memory cell subsets is the potentially circular nature of definitions. For example, because mutation is accepted as a marker for human memory B cells, this of course makes it impossible to identify unmutated memory cells, should they exist (6, 22). It is most desirable to have a definition of memory B cells based on biology alone, and then to assess the markers of such cells.

To begin to address these issues, we have developed a system that generates large numbers of murine memory B cells. Our approach uses a B cell receptor (BCR) H chain transgenic (Tg; Vh186.2), which, in combination with endogenous λ_1 L chain, encodes a receptor specific for the hapten 4-hydroxy-3-nitrophenyl (NP) (23). In such mice, the precursor frequency is elevated to ~2% of B cells, which is higher than the 0.02% in non-Tg mice (12), but not so high as to inhibit immune responses, as is observed in monoclonal Tg mice (24). At the peak of the GC response in our mice, ~15% of splenocytes are NP-specific B cells (25). This strong response leads to large numbers of residual Ag-specific B cells at >12 wk after immunization (26), the excess of which compared to sham-immunized mice can reasonably be assumed to be memory cells. Depending on the specific Tg system and the immunization protocol, residual Ag-specific cells could number as many as 12×10^6 per spleen 12–16 wk after immunization, which is ~10-fold more than the preimmune state (unpublished data).

Further, we have shown in this system that short courses of BrdU durably labeled a subset of Ag-specific B cells that remains stable for at least 20 wk after immunization (26). Using BrdU, we defined memory B cells as Ag-specific cells that divided in response to Ag (and thus took up BrdU), and then exited the cell cycle and remained in a resting state (and thus retained the BrdU) for >3 mo after immunization. We found that such Ag-specific BrdU$^+$ cells were at least sixfold more numerous in immune compared with alum-immunized mice (26). This definition of memory cells is appealing because it avoids assumptions about markers or sites of development, only requiring that the cell had divided in response to Ag and remained in the animal for a long duration thereafter.

We use this approach to define the expression of a large panel of surface and intracellular markers on murine memory B cells, allowing us to define a unique phenotype. Interestingly, we found that memory cells display considerable phenotypic heterogeneity. Notably, some subsets of cells that clearly had responded to Ag months ago, including cells that had undergone isotype switch, remain unmutated. By studying mutational content over time in one of the subsets, we found an enrichment of replacement mutations as the memory compartment aged, suggesting ongoing selection or initial imprinting of longevity in higher affinity B cells. Finally, we determined by immunohistology that although BrdU-labeled, Ag-specific memory B cells were found in the marginal zone (MZ), as reported (27, 28), they did not preferentially localize there, in contrast to commonly held assumptions.

RESULTS

Several surface markers distinguish murine memory B cells from their naive counterparts

Although NP-immune Vh186.2 H Tg mice have substantial increases in the Ag-specific (4-hydroxy-3-nitroiodophenyl [NIP]-binding) population, to unambiguously label memory cells, we injected both alum-treated and NP-immunized mice with BrdU during the peak of the GC response (25, 26). This BrdU pulse-labeling strategy durably marked those cells that derived from dividing precursors and then stopped cycling during or immediately after the labeling period. Such cells meet a stringent definition for memory as used by us and others (29–31). Note that only a fraction of memory cells are labeled by this strategy because cells that differentiated before and after the short labeling window would not take up BrdU. Our previous studies showed that immunization with Ag versus alum alone yielded, on average, a fivefold enrichment (range four- to sevenfold) in the frequency and number of BrdU$^+$ cells in the Tg mice, which is the product of the frequencies of B220$^+$/NIP$^+$ and NIP$^+$/BrdU$^+$ cells (Fig. 1 A) (26). This allowed us to identify proteins that were increased in expression on BrdU$^+$ cells, as at least 80% of them would be true memory cells, i.e., elicited only after exposure to cognate Ag.

We conducted a comparative FACS survey of 29 markers on NP$^+$ B cells from naive mice and NP$^+$/BrdU$^+$ B cells from immune (m+s)Ig Tg mice (see references [25, 26] and Materials and Methods for details on the mice). Most of the markers examined did not show significant differences between naive NP$^+$ and memory NP$^+$/BrdU$^+$ cells (P > 0.05; Table I). However, there were some notable exceptions (boldface in Table I), indicating that memory differentiation resulted in subtle, but definite, changes of the naive B cell phenotype. Each of these differentially expressed molecules will be described in detail in the following sections.

A greater proportion of long–lived B cells express high levels of CD80 after immunization

There was a significant increase in the frequency of CD80$^+$/NP$^+$/BrdU$^+$ B cells in immune mice compared with NP$^+$ B cells from alum-immunized (m+s)Ig Tg mice (P > 0.005; Fig. 1 B and Table II). There was a bimodal distribution of CD80 on NP$^+$/BrdU$^+$ and total NP$^+$ B cells from immune mice (Fig. 1 B and not depicted). To determine if increased expression of CD80 was a general characteristic of murine memory B cells, we generated NP-specific memory B cells in four other distinct systems (Fig. 1 C and Fig. S1, available at http://www.jem.org/cgi/content/full/jem.20062571/DC1): non-Tg C57BL/6J (B6) mice, mIg Tg mice that were immunized
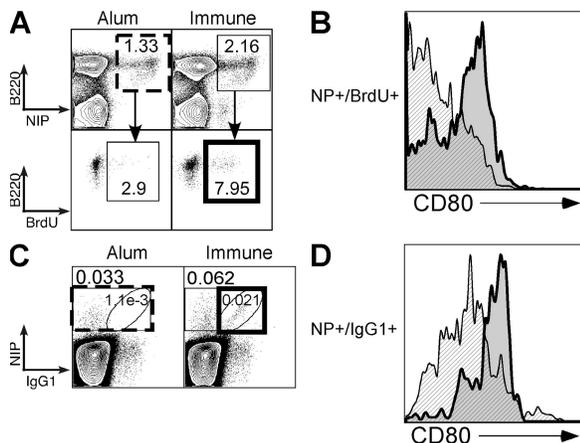
Figure 1. A greater proportion of memory B cells are CD80+ than naive B cells. (A) Representative FACS plots of alum- and NP-immunized (m+s)Ig spleen cells stained with B220 and NIP-PE (top row) and B220 and anti-BrdU (bottom row) 12 wk after immunization. The plots on the bottom row are gated on the NP+ population from the top row, as indicated by the arrows. For comparisons of cell surface markers, total NP+ B cells from naive mice (gate with dashed line) and NP+/BrdU+ B cells from immune mice (gate with bold line) were used. (B) The level of CD80 on naive NP+ B cells (hatched histogram with thin line) and immune NP+/BrdU+ B cells (darkly shaded histogram with bold line) 8 wk after immunization (representative histogram from three mice per group). (C) FACS plots of alum- and NP-immunized B6 spleen cells gated on CD19+ B cells and stained with NIP-APC and anti-IgG1 15 wk after immunization. The percentage of total NP-binding cells of B cells is shown, as well as the percentage of IgG1+/NP+ cells. (D) The level of CD80 on NP+ B cells from alum controls (hatched histogram with thin line) and NP+/IgG1+ B cells from immune mice (darkly shaded histogram with bold line) 15 wk after immunization (representative histogram from five mice per group).

twice (25, 26), mIg Tg cells transferred to an immunized irrelevant recipient, and immunized B1-8 knock-in mice (32). In each case, CD80 expression was increased on a subset of memory B cells (Fig. 1 D and Fig. S1, A–C). Notably, in stains that produced isotype-switched memory B cells, most IgG1+/NP+ cells were CD80+ (Fig. 1 D) and, conversely, most CD80+ cells were IgDneg (Fig. S1, C and D). Thus, CD80 is upregulated on memory cells from Tg and non-Tg mice, on both IgM and IgG cells, as detected in intact mice or after transfer, with or without BrdU.

The lack of up-regulation of CD80 on some memory cells, which is a feature of each of these systems, could not be attributed to contamination of memory cells with naive CD80neg/NP+ cells because even in situations in which >90% of the NP+ population was generated via immunization, almost half of the NP+ cells were nonetheless CD80neg (Fig. 1 D and Fig. S1, B and D). Thus, the existence of CD80+ and CD80neg populations seems a general feature of the memory B cell compartment. These data parallel findings of a subset of human CD27+ cells with higher levels of CD80 (8, 18–20).

Other cell surface markers that distinguish memory and naive B cells

There were significant differences in the expression of four additional cell surface markers in NP+/BrdU+ cells from immune Vh186.2 Tg mice compared with NP+ cells from the following alum-immunized mice: MHC class II (MHCII), CD95, CD62L, and CD73 (P < 0.02; Fig. 2 A and Table II). These changes were reflected in an increased frequency of positive cells, an increased level of expression among the positive cells, or both. There was a twofold increase in frequency of CD95+/NP+/BrdU+ cells versus naive CD95+/NP+ cells (Table II), although among the CD95+ population, the levels of CD95 on NP+/BrdU+ cells and NP+ naive cells were similar (Table II, MFI). Similarly, there was an increased frequency of CD73+ cells among immune NP+/BrdU+ cells (Fig. 2 A and Table II). Again, the up-regulation of these two markers was confirmed on NP+/IgG1+ cells in both the B1-8 knock-in and the non-Tg B6 mice (Fig. 2, B and C). These data extend to the protein level a previous report of increased CD95 mRNA expression in non-Tg IgG1+/CD38+/NP+ memory cells versus naive CD38+ B cells (12). Interestingly, multicolor flow cytometry showed that CD80 and CD73, both of which are found on only a subset of memory cells, are up-regulated on the same subpopulation; there is also a CD80+/CD73neg population that is most apparent among IgG1+ memory cells in B1-8 knock-in and B6 mice (Fig. S2, available at http://www.jem.org/cgi/content/full/jem.20062571/DC1). MHCII expression showed a different pattern, with a significant increase in the mean fluorescence intensity (MFI) of MHCII expression on NP+/BrdU+ compared with naive NP+ cells (P < 0.005). This was caused by a shift in the distribution

Table I. List of surface markers used to determine differences between immune NP+/BrdU+ B cells and naive NP+ B cells

Adhesion/ migration	Costimulatory/proliferation	Apoptotic/survival	Lineage	Fc-, cytokine-, and complement receptors
CD43	CD40	Bcl-XL	*CD24*	PIR-A
VLA-4	CD45RB	Bcl-2	BLA-1	CD124
LFA-1	Ly6C	**CD95**	*CD38*	CD127
ICAM-1	Ly6A/E	***CD73***	**MHCII**	*CD35*
CD11b	CD27			*CD23*
CD44	CD19			
CD62L	CD22			
	CD86			
	CD80			

Markers that are bold are different between naive and memory cells. Those that are italicized are heterogeneously expressed.

Table II. Frequency (percent positive) and MFI values for cell surface markers that differed between memory and naive B cells

| | Naive NP+ | | Immune NP+/BrdU+ | |
	Positive[a]	MFI[b]	Positive	MFI
	%		%	
CD80	24.7 ± 2.4	21.0 ± 0.3	63.7 ± 2.6	38.5 ± 1.7
CD95	33.3 ± 4.9	31.0 ± 0.3	60.1 ± 1.8	32.9 ± 2.0
CD73	30.9 ± 4.1	1,103 ± 45.6	67.1 ± 2.7	1,096 ± 65.0
Class II	98.4 ± 0.3	131 ± 1.3	99.4 ± 0.3	206 ± 11.6
CD62L	54.4 ± 2.3	347 ± 13.5	76.8 ± 1.5	465 ± 19.1

[a]For each cell surface marker, the mean frequency of the population that was positive, as well as the MFI of the positive population, is reported for each group. $n = 3$–8 mice per group from 1–2 experiments.
[b]Calculated from the gated positive population for each marker.

of NP+/BrdU+ cells to the highest expression levels of MHCII (Fig. 2 A and Table II). There also was a significantly increased population of CD62L^hi cells among the NP+/BrdU+ B cells (P < 0.01; Fig. 2 A and Table II). We did not test for the modest increases in these two markers in the two IgG1-producing systems.

Some proteins were heterogeneously expressed in both memory and naive subsets, indicating possible heterogeneity in function

There were no significant differences in expression between the naive and memory populations among the remaining 24 molecules (P > 0.05; Table I). However, there were a few that displayed bimodal expression, yet in a similar pattern in both the naive and memory compartments, as seen in CD23,

CD35, and CD38 (Table I and Fig. 2 D). CD35 is particularly interesting because follicular and MZ B cells are usually distinguished by their relative expression of this surface receptor (follicular B cells are CD35^lo and MZ B cells are CD35^hi [reference 33]). Given this paradigm, it was surprising to see continued heterogeneity of CD35 expression in the memory compartment (Fig. 2 D). Memory B cells are reported to reside in the MZ (Fig. 6) (27, 28), although it is unclear if they necessarily express markers of the naive resident MZ B cell population, such as CD35. Regardless, heterogeneous expression of cell surface markers such as CD35 suggested either diverse origins or functions of long-lived B cells, or both. Notably, because our system restricts the precursor and memory populations to essentially a single BCR, this heterogeneity is independent of BCR specificity.
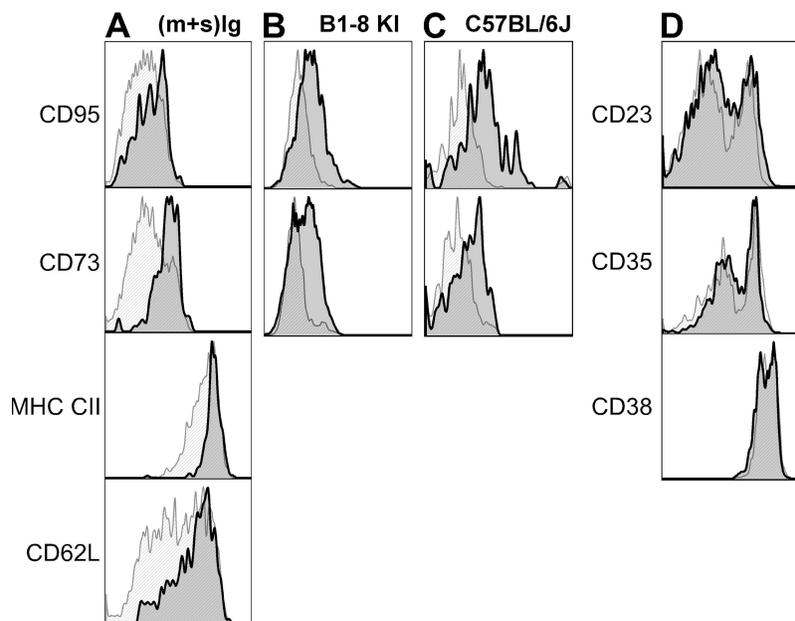
Figure 2.   There were several surface markers that exhibited differences between naive and immune NP+ B cells. Markers that were significantly different between naive and memory B cells from (m+s)Ig Tg (A), B1-8 knock-in (B), and B6 mice (C). Total NP+ B cells from alum control mice (hatched histogram with thin line) and NP+/BrdU+ B cells (A) or NP+/IgG1+ B cells (B and C) from immunized mice (darkly shaded histogram with bold line) were compared 16–20 wk after immunization. (D) Markers that were not different, but presented a heterogeneous pattern in both naive and memory NP+ cells from (m+s)Ig mice are shown. Each histogram corresponds to one representative mouse out of three to seven total mice per group.

Bimodal distribution of somatic mutations among CD80^{+} memory cells

CD80^{+}, and not CD80^{neg}, memory B cells represent the mutated compartment. Given the heterogeneous expression of CD80 among memory B cells, we were interested in whether this marker correlated with any other functional or genetic properties. Mutations are an indication of prior activation, e.g., in the GC (34), from which most memory cells are assumed to originate (29). Thus, V gene mutation is generally considered a hallmark of memory B cells. We wanted to determine if the presence of mutation correlated with expression of CD80. For these studies, it was not feasible to use BrdU as a marker for long-lived memory cells because its detection requires DNase treatment, which inhibits amplification of V region DNA sequences. Therefore, we used FACS-based sorting to purify CD80^{+} and CD80^{neg} NP^{+} B cells from (m+s)Ig Tg spleens taken 24 wk after immunization, a time at which λ^+ GC B cells are no longer detectable in spleen (Fig. S3, available at http://www.jem.org/cgi/content/full/jem.20062571/DC1), and sequenced the endogenous $V\lambda_1$ genes (Fig. 3 A). A greater number of mutations per $V\lambda_1$ gene was observed in the sequences recovered from CD80^{+} versus CD80^{neg} cells (Fig. 3 B; P = 0.003, Mann–Whitney test). The increase in the mean number of mutations per $V\lambda_1$ gene of CD80^{+} sequences was caused by both a higher frequency of mutated sequences and a greater extent of mutations per individual sequence (Fig. 3, C and B, respectively). Although the frequency of germline sequences was significantly lower in the CD80^{+} population (P = 0.008, χ^2 test), such sequences still made up 30% of the total number from this otherwise highly mutated population (Fig. 3 C).

Among CD80^{+} cells, mutations are restricted to the CD35^{lo} compartment. Given the heterogeneity in the extent of mutation even in the CD80^{+} population, along with the observation that there was a bimodal distribution of CD35 expression among memory cells, we next asked whether mutations would segregate with CD35 expression (Fig. 4 A). Strikingly, among the CD80^{+} cells, the mutated sequences were highly enriched in the CD35^{lo} population (Fig. 4, B and C; P = 0.001, Mann–Whitney). Moreover, even the few mutated sequences in the CD35^{hi} subset had only 1–2 mutations, whereas the average mutated sequence from CD35^{lo} cells had ~4 (Fig. 4 B and not depicted). The absence of mutation in the CD80^{+}/CD35^{hi} population was surprising considering that CD80—regardless of CD35 expression—appears to be a specific marker for memory B cells.

Although there is the possibility of some naive cells being sorted in the CD80^{+}/CD35^{hi} gate, even in immune mice, this is not sufficient to account for the striking lack of mutations in CD80^{+}/CD35^{hi} cells. Naive cells only account for 25–30% of the CD80^{+} population in immune mice, and of the CD80^{+} compartment in naive mice, 70% are CD35^{hi} (unpublished data). This results in 28% of CD80^{+}/CD35^{hi} cells being naive in immune mice. Therefore, at most, 30%
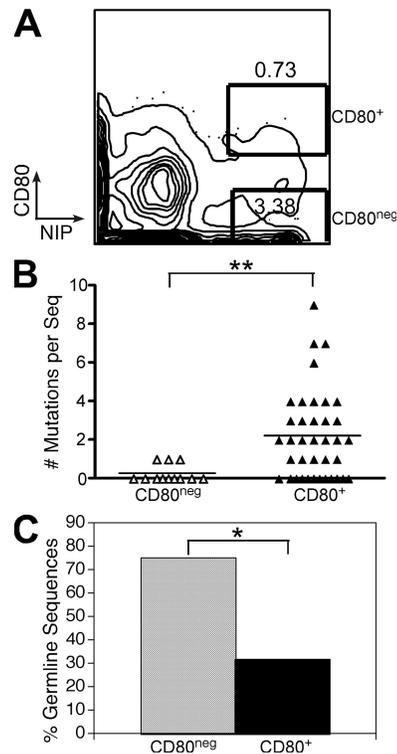
Figure 3. CD80^{+}/NP^{+} B cells contain most of the mutations found in the V regions of the λ_1 gene from immune (m+s)Ig mice. (A) Sort profile from (m+s)Ig mice immunized 24 wk before. Gates were set on NP^{+}/CD80^{+} and NP^{+}/CD80^{neg} cells based on staining from alum-treated mice, which lacked a significant CD80^{+} population. (B) Closed triangles represent the number of mutations in individual λ_1 genes from the CD80^{+} population ($n = 38$), and open triangles represent the number of mutations from the CD80^{neg} population ($n = 12$). **, P < 0.005, Mann–Whitney test. (C) The percentage of sequences in germline configuration out of the total number of sequences obtained from CD80^{+} (shaded bar) and CD80^{neg} (hatched bar) NP^{+} cells. *, P < 0.01, χ^2 test.

of the sequences could potentially originate from unmutated naive B cells with intrinsically high levels of CD80 in the CD35^{hi} compartment. Contamination from unmutated naive cells cannot, therefore, completely account for 73% of the sequences in the immune CD80^{+}/CD35^{hi} population being germline (Fig. 4 C). Importantly, in BrdU labeling experiments, there was an equal frequency of BrdU^{+} cells in the CD80^{+}/CD35^{lo} and CD80^{+}/CD35^{hi} populations, indicating that both compartments are generated equally during the GC phase of the response, and thus both contain true memory cells (unpublished data).

To determine more definitively the mutation status of CD80^{+}/CD35^{+} memory cells, and to extend the findings to wild-type non-Tg mice, we sorted these populations from immune B6 mice 13, 14, and 15 wk after immunization, using IgG1, along with CD80, to identify memory cells and NIP-binding to identify Ag-specific cells (Fig. 4 D). In these sorts, the frequency of NIP[+]/IgG1 cells was ~50 cells per 10^6 splenocytes, which is in agreement with a prior study using the same Ag in B6 mice at 11.5 wk (12). The latter study
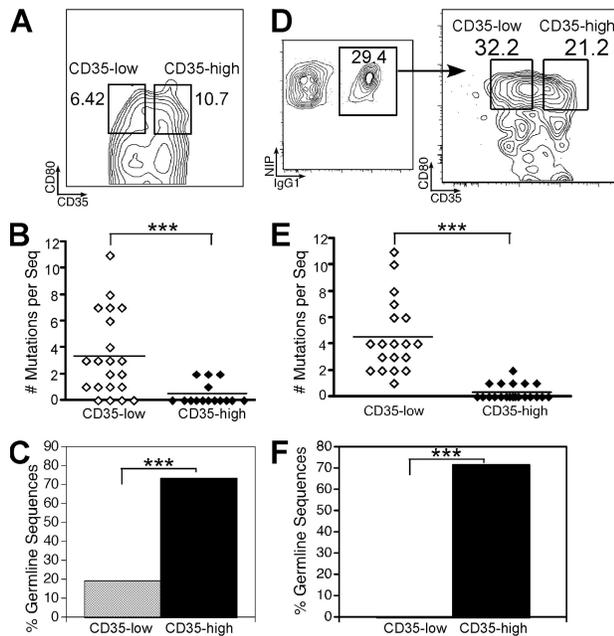
Figure 4. CD35^{lo}/CD80$^+$/NP$^+$ B cells contain most of the mutations found in the V regions of the λ_1 gene from immune (m+s)Ig and non-Tg B6 mice. NP$^+$/CD80$^+$ cells were further sorted based on CD35 expression. Shown is the total NP$^+$ B cell population from immune (m+s)Ig Tg (A) or non-Tg B6 splenocytes (D); the CD80$^+$/CD35^{hi} and CD80$^+$/CD35^{lo} gates (with frequencies) used for sorting are shown for each strain. (B and E) Closed diamonds represent the number of mutations in individual λ_1 genes from the CD80$^+$/CD35^{hi} population ($n = 15$ [m+s]Ig Tg; $n = 21$ B6), and open diamonds represent the number of mutations from the CD80$^+$/CD35^{lo} population ($n = 21$ [m+s]Ig; $n = 19$ B6). ***, $P < 0.001$, Mann–Whitney test. (C and F) The percentage of sequences in germline configuration out of the total number of sequences obtained from CD80$^+$/CD35^{hi} (shaded bar) and CD80$^+$/CD35^{lo} (hatched bar) NP$^+$ cells from both mouse strains. ***, $P < 0.001$, χ^2 test.

also found only 4 NP$^+$ GC cells per 10^6 splenocytes at this time point, indicating little contamination by persistent GC cells (albeit with cells that would have much higher mutation frequencies in any case [reference 12]) could not affect the results. We also confirmed in these sorts that essentially all isolated cells were CD38^{hi} (Fig. S4, available at http://www.jem.org/cgi/content/full/jem.20062571/DC1), further showing that they were not GC cells (14). In a striking parallel to the results from the (m+s)Ig strain, the CD80$^+$/CD35^{lo} subset was more highly mutated than the CD35^{hi} subset of IgG1$^+$/NP$^+$/CD38$^+$ B cells from immune B6 mice (average 4.5 mutations/sequence vs. 0.33 mutations/sequence, respectively; Fig. 4, E and F). The difference in mutation status between the subsets was quite remarkable, as there were no unmutated sequences recovered in the CD80$^+$/CD35^{lo} population (Fig. 4 F), and of the mutated sequences in the CD80$^+$/CD35^{hi} group, only 1–2 mutations were observed (Fig. 4 E). Thus, the few unmutated sequences found in sorted CD80$^+$/CD35^{lo} immune (m+s)Ig NP$^+$ cells most likely were the result of naive contamination, which has been effectively eliminated in the sorts using IgG1 in B6 mice.

We conclude that expression of CD80 in combination with low expression of CD35 distinguishes the mutated population of memory cells, with high expression of CD35 conversely identifying a previously unappreciated population of unmutated memory cells.

Selection of mutated sequences over time during the late primary response

To determine whether these memory subsets had differential survival or selection, we next asked whether the distribution of mutations was altered as the memory compartment aged. Comparing Vλ_1 sequences from the CD80$^+$/NP$^+$ population obtained 12 and >24 wk after immunization in (m+s)Ig Tg mice, we found more mutations per Vλ_1 gene in the sequences obtained at >24 versus 12 wk (Fig. 5 A; $P < 0.05$, Mann–Whitney test). In principle, this could either be caused by ongoing mutation in the memory compartment or by selective survival of mutated cells. Ongoing mutation is not an explanation, however, as there was no further accumulation of mutations in the mutated sequences at 24 vs. 12 wk (Fig. 5 A and not depicted). Rather, the overall increase in mutations per gene in the sequences from >24-wk-old memory cells was accounted for by a significant reduction in the fraction of unmutated sequences at >24 versus 12 wk after immunization (Fig. 5 B; $P < 0.02$, χ^2 test). Thus, it appeared that B cells with mutated V regions were being selectively preserved over time, although these V regions did not accumulate any further mutations.

The loss of unmutated sequences at later times indicated a selection process either for cells that contain mutated sequences (positive) or against those cells that contain unmutated Ig genes (negative). Although it was not possible to distinguish these possibilities, differences in the selection of the mutated sequences could be measured over time, analyzing the relative distribution of replacement mutations in the complementarity-determining regions (CDRs) and framework regions (FWs) of Ig V regions (35, 36). Positive selection tends to enrich replacement mutations in the CDRs (36). Interestingly, the relative distribution of replacement mutations in the CDR and FW regions changed significantly with time (Fig. 5 C; $P = 0.0016$, χ^2 test). Although 59% of replacement mutations were in the CDRs 12 wk after immunization, >85% of replacement mutations were in CDRs at >24 wk after immunization. Thus, enrichment of mutated sequences over time in the memory compartment is accompanied by positive selection of replacement mutations in CDRs.

Memory cells are equally distributed between the follicle and MZ in spleen

Memory B cells are thought to reside in the MZ of the spleen, though in the rodent this conclusion is based on a study of rat immune responses at relatively short time periods after immunization (2–4 wk; [references 28, 37]). In humans, V genes microdissected from the splenic MZ carried somatic mutations, suggestive of memory cells (27). Human CD27$^+$ memory B cells also have a MZ-like phenotype, which is
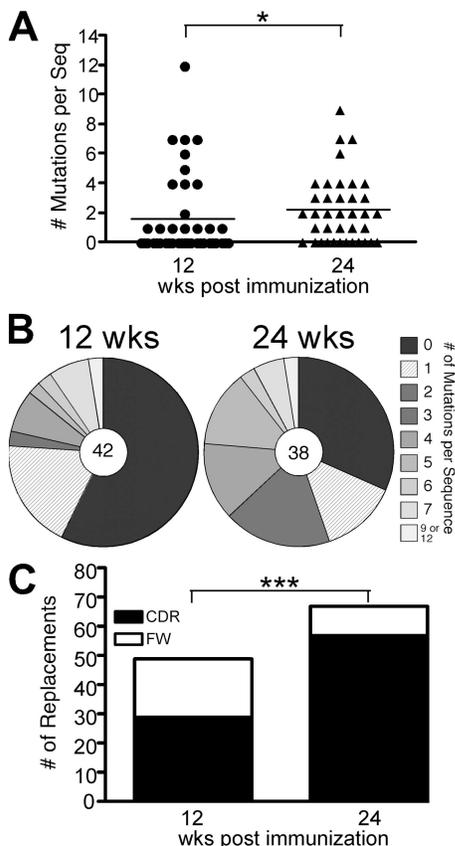
Figure 5. A loss of unmutated cells 12–24 wk after immunization suggests ongoing selection of the mutated memory compartment. CD80$^+$/NP$^+$ B cells were sorted from (m+s)Ig mice 12 and 24+ wk after immunization. (A) Circles represent the number of mutations in individual λ_1 genes from the CD80$^+$ population 12 wk after immunization ($n = 42$), and triangles represent the number of mutations from the CD80$^+$ population 24+ wk after immunization ($n = 38$). *, P = 0.04, Mann–Whitney test. (B) The distribution of sequences with the indicated number of mutations is shown. The total number of sequences is shown in the center circle. P < 0.05, χ^2 test. (C) The distribution of replacement mutations in either the CDR (black) or FW (white) regions of the Vλ_1 at 12 and 24 wk after immunization is shown. ***, P < 0.005, χ^2 test.

CD35^{hi}/CD23^{lo} (10, 22, 38). We used a combination of immunohistochemistry and fluorescence to identify the BrdU$^+$/λ^+ memory cells in the MZ and follicle of the spleen at 8 and 12 wk after immunization in mice given a BrdU pulse label during the peak of the immune response. The inner border of the MZ and the outer border of the follicle were demarcated with MOMA-1 (39). The outer border of the MZ was marked using F4/80, which stains macrophages from the red pulp, such that the unstained area between the MOMA-1 ring and the F4/80-stained red pulp is the MZ (Fig. 6, A and D). To identify Ag-specific memory B cells, we used Abs to the λ light chain, which in the context of the expressed Vh186.2 gene confers specificity for NP (Fig. 6, B and E). BrdU$^+$/λ^+ cells were identified from images taken at higher magnification (400×; Fig. 6 E, insets) and their position in either the follicle or MZ was determined from over-

laid images, as in Fig. 6 D (see Materials and methods for details). Cell counts in either the follicle or MZ were normalized to the measured area of the region analyzed, and the ratio of the normalized counts in the follicle and MZ was determined (Fig. 6 F). We found that Ag-specific memory B cells were equally distributed between the follicle and MZ at 8 wk after immunization. This distribution evolved with time, as the density of λ^+/BrdU$^+$ cells in the follicle at 12 wk after immunization was twofold higher than that in the MZ (Fig. 6 F; P = 0.03, Student's t test).

It has been thought that CD35 expression correlates with anatomical position in the spleen, i.e., CD35^{hi} B cells in the MZ (33), although this has never been determined directly for memory B cells. To determine the expression of CD35 on BrdU$^+$/λ^+ cells located in either the follicle or MZ, an analysis similar to that described in Fig. 6 was performed, with the addition of immunofluorescent staining for CD35, allowing for distinction between CD35 bright and dull cells. In a limited study, we found that approximately half of the BrdU$^+$/λ^+ B cells in the follicle 8 wk after immunization expressed high levels of CD35 (unpublished data). This suggested that for the memory compartment, in contrast to preimmune B cell subsets, high expression of CD35 did not necessarily correlate with localization to the MZ.

DISCUSSION

The studies reported here provide several new insights into the biology of memory B cells. We established a system to identify memory B cells with a minimum of a priori assumptions that defined new phenotypic markers for memory cells and, in the process, revealed unexpected heterogeneity, including unmutated memory cells. Finally, we found that memory cells are located in both the follicle and MZ of the spleen. The approach and the markers it identified should be useful for the study of murine memory B cells in a variety of systems.

Although many surface markers were similarly expressed between naive and memory cells, as expected from two resting populations in the same cell lineage, we did find substantial and reproducible differences for a small number of markers. That we found unique surface marker expression patterns strongly supports the conclusion that we have, indeed, identified discrete populations of memory B cells. Consistent with studies done in both humans and mice (12, 18–20), we observed an increase in CD80$^+$ and CD95$^+$ cells among the memory B cell population compared with the naive population (Fig. 1, Fig. 2, and Fig. S1, available at http://www.jem.org/cgi/content/full/jem.20062571/DC1). Up-regulation on memory cells of the most important surface proteins—CD73, CD80, and CD95—was found not just on IgM$^+$/NP$^+$/BrdU$^+$ cells from Vh186.2 Tg mice, but also on IgG1$^+$/NP$^+$ cells in B1-8 knock-in and in non-Tg B6 mice. This confirms the generality of these markers, as well as validates the relevance of the Vh186.2 Tg and B1-8 knock-in systems. Other surface proteins differentially expressed on memory cells in human, most notably CD27 and CD23, were not different between murine naive and memory B cells
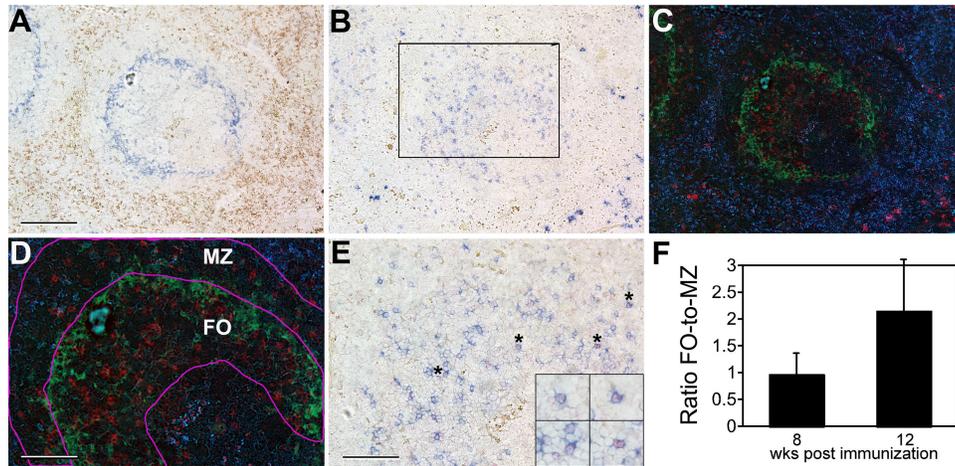
Figure 6. Memory cells are equally distributed among the follicles and MZs of the spleen. Serial sections from a (m+s)Ig spleen 12 wk after immunization were stained with anti–MOMA-1 (blue)/anti-F4-80 (red) (A) and anti-λ(blue)/anti-BrdU (red) (B) Abs. The portion magnified in E is boxed in B. (C) Images of the histochemically stained sections were inverted and false colored in Photoshop, and serial sections were overlaid using architectural landmarks as guides (blue, F4-80; green, MOMA-1; red, λ). (D) The area bounded by the pink lines was measured and used to determine the density of BrdU$^+$/λ$^+$ cells within each region. (E) BrdU$^+$/λ$^+$ cells (marked by asterisks) were counted from 200× images, and their location was determined from the images generated in D. Inset, 400× magnified images of four BrdU$^+$ cells (pink nuclei) costained with anti-λ (blue surface stain). (F) The relative ratio of λ$^+$/BrdU$^+$ cells in the follicles and MZs of the spleen was calculated for 8 and 12 wk after immunization. Mean values were calculated from five to six different follicle and MZ regions at each time point. Error bars represent the propagated error of the mean of each ratio. Bars: (A–C) 1 mm; (D and E) 500 μm.

and likely represent species differences (Fig. 2 and not depicted). CD73, MHCII, and CD62L had increased expression on memory cells; none of these had been identified previously in human or mouse. A homogenous shift in expression was seen for CD95, CD62L, and MHCII, albeit with some overlap with naive populations, such that neither of these markers alone should be used to identify memory cells. However, there is heterogeneity of expression of CD80 and CD73 (Fig. S2), such that a subpopulation of positive cells clearly emerges in the memory compartment. Yet there are also substantial fractions of BrdU$^+$ Ag-specific cells that have low expression of these markers. Thus, CD80 and CD73 together do delineate a separable population that includes a fraction of all memory cells.

Collectively, the increased levels of CD80 and MHCII on memory B cells suggest that these cells would differentially engage CD4 T cells (either naive or memory) during a recall response. A variety of further genetic studies will be required to test this hypothesis. In this vein, although B cells are generally presumed to be less potent APCs for naive T cells compared with DCs, the experiments that have demonstrated this effect have used naive, resting B cells (40, 41).

It is more difficult to speculate on the roles of CD95 and CD73. Although one might expect that memory cells would be more susceptible to FasL–induced cell death mediated by activated Th1 T cells, CD95 expression does not always correlate with sensitivity to ligation-mediated cell death (42). CD73 is an ectoenzyme that generates extracellular adenosine, and which has been linked to down-modulation of inflammatory immune responses (43). Interestingly, CD73 was previously noted to be more highly expressed on isotype-switched

BALB/c B cells, which is consistent with our findings (44), although little is known about its specific role in B cells.

Although naive NP$^+$ B cells had both CD62L^{lo} and CD62L^{hi} populations, memory NP$^+$/BrdU$^+$ B cells were more homogenously CD62L^{hi}, which is reminiscent of a central–memory phenotype in T cells (Fig. 2) (21). Memory T cells that lack CD62L are more likely found in peripheral tissues (21, 45). Therefore, it is possible that CD62L^{lo} memory B cells could be recirculating in the periphery, and therefore absent from the spleen, providing an explanation for the difference in expression profiles between naive and memory B cells. In fact, NP$^+$/BrdU$^+$ B cells could be found in peripheral organs of immune mice, such as the liver and intestine, although the expression of CD62L on these cells was not determined (unpublished data).

Among our most interesting findings was phenotypic heterogeneity in the memory compartment, e.g., as defined by expression of CD35 and CD80 (Figs. 1 and 2). Although this approach to subsetting memory cells is new, there have been other demonstrations of heterogeneity in the memory B cell compartment, particularly in regard to the Ig isotype (46). In humans, IgM and IgG subtypes of CD27$^+$ memory cells have been delineated and shown to have some different functional properties (2, 47). Similarly, in human, CD148 identifies memory cells, only a subset of which is positive for the more typically used marker CD27 (20).

We assessed memory B cell subpopulations for V region mutation. Many sequences from CD80$^+$ memory B cells were substantially mutated, whereas CD80^{neg} B cells from immune (m+s)Ig mice were mainly unmutated (Fig. 3). There is heterogeneity within the CD80$^+$ population itself,

which was a mixture of mutated (70%) and germline (30%) sequences. These mutated and unmutated CD80$^+$ populations could be further separated by their expression of CD35, with mutated cells found principally in the CD80$^+$/CD35^{lo} subset (Fig. 4). Importantly, we extended these findings to non–Tg B6 mice, demonstrating that among IgG1$^+$/CD80$^+$/CD38$^+$ memory cells, essentially all the nonmutated sequences were found in the CD35^{hi} subset. Thus, we have clearly identified a novel and substantial population of memory B cells that is isotype switched, but develops without accumulation of mutations. A similar frequency of unmutated cells was evident in the IgG1-expressing memory compartment of B6 NP-immune mice in a prior study, although this aspect was not commented on, nor was it identified as being confined to the CD80$^+$/CD35^{hi} subset of memory cells (12). Interestingly, there may be a parallel in humans, as there is a fraction of unmutated memory B cells in the CD27$^+$ memory population (5 germlines out of 67 sequences [reference 6]).

The origins of these mutated and unmutated subsets of memory cells are unclear. Classically, memory B cells are thought to derive from the GC, where most mutation of Ig genes is known to occur (29, 34). However, recent studies suggest that there could be at least one, if not multiple, GC-independent pathway of memory development and selection. In B6 mice, whereas GC B cells demonstrated a steady increase in the number of mutations over time, memory cells retained the same lower frequency up to 160 d after immunization (12). This disconnect between the extent of mutation in the two compartments implied that a substantial portion of selection into the memory pool either occurred independently of the GC reaction or occurred very early in the GC, before significant mutation took place. Subsequent studies involving genetic deficiency of CD40 and Bcl-6 in human and mouse, respectively, demonstrated that in the absence of GCs, an unmutated, functional memory B cell compartment could develop (48, 49). Additionally, in mice expressing a β-gal reporter that marks cells that have undergone GC differentiation, the responding population during a secondary challenge was a mixture of β-gal$^+$ and β-gal^{neg} B cells (50). This implied that cells could participate in memory responses, even if they had not entered the GC during the primary response, although this study could not distinguish whether the responding β-gal^{neg} B cells had seen Ag previously or were naive, partly because of incomplete marking of GC cells (50). Recently, it has also been shown that T-independent responses can produce long-lasting, functional memory B cells, which appear to be phenotypically distinct from T-dependent memory B cells and comprise a significant portion of the "natural" memory population (31, 51, 52). The exact details of these novel pathways of memory B cell selection have yet to be elucidated. Nonetheless, our data show that even with a defined Ag and a defined, genetically homogenous responding population, phenotypic heterogeneity can still be generated in a T-dependent response.

Although little is known of the functional significance of these different memory pathways and the cells they gener-

ate, differences could be predicted by differences in expression of known surface markers, like CD35 and CD80, which are likely to be important for memory B cell function upon reimmunization. In this regard, one potentially significant observation was that mutated cells were progressively enriched among the CD80$^+$ Ag-specific cells over time (Fig. 5). Several possible explanations can be entertained for this enrichment, as follows: (a) unmutated cells have a shorter half-life and are not homeostatically renewed in the memory compartment as efficiently as the mutated cells; (b) some of the unmutated cells lose expression of CD80, but remain as memory cells with a different phenotype; and (c) the unmutated CD80$^+$ cells have a greater tendency over time to localize in compartments outside the spleen, and thus would have been invisible to our assay. It seems likely, however, that selective survival must play at least some role. Otherwise, it would be difficult to explain the enrichment of replacement mutations in CDR that is also seen among the mutated subset over time (Fig. 5). This observation suggests that affinity itself plays a role in long-term survival. Affinity-dependent survival capacity could be imprinted at the time of initial selection or result from continued sensing of residual Ag in the alum depot or in retained immune complexes. "Tonic signaling," a term that refers to low-level BCR stimulation, clearly does promote survival of naive B cells (32, 53), and thus sensing of very low levels of residual Ag as a mode to promote memory survival would be entirely analogous.

Finally, we observed that Ag-specific BrdU$^+$ memory cells were found in both the follicle and the MZ. This was unexpected because, on the basis of studies in rats by MacLennan et al., it had been widely assumed that memory cells were only to be found in the MZ (28). Actually, data from those studies (as mentioned by the authors themselves) demonstrate that some memory cells were indeed found in the follicle. These MZ localization data were mainly derived from time points shortly after immunization (28). We found relatively more memory cells located in the follicle with time after immunization (Fig. 6 F). It is still not clear if the discrepancy between our results and the studies in rat relate to species differences, timing of observation, methods used to identify memory cells (in [reference 28], only Ag specificity was used) or even the nature of immunogen. In any case, our data call for a reexamination of the notion that memory cells are exclusively or even mainly located in the MZ in mice.

A related question is whether memory cells with the CD35^{hi} "MZ" phenotype (33) only reside within the MZ. We attempted to assess this using BrdU and immunofluorescence for CD35, in hopes of identifying whether follicle or MZ memory B cells had different levels of expression of this marker. Although it proved technically too challenging to rigorously quantitate the distributions of CD35^{hi}/BrdU$^+$ cells, it was clear that follicles did indeed contain some cells that were CD35^{hi}. From this, we conclude that in memory cells CD35 expression levels are not indicative of microanatomic localization.

We have established the existence of subsets of memory B cells using a Tg mouse model, a Vh knock–in model, and non–Tg mice. That we could observe generation of different types of memory cells, even with a starting population that expressed a single type of BCR, favors the notion that stochastic factors can generate functional heterogeneity in the memory compartment. We believe this system demonstrates at least some of the biological capabilities of memory cell generation. However, we recognize that this hapten–specific system, although having strengths and enabling possible pathways to be defined, may not be indicative of every situation. In pathogen responses, or with other antigens and innate immune signals, the direction of differentiation could be altered, leading to the domination of one or another type of memory cell. Now that such subsets and their associated markers are identified, it will be possible in future work to elucidate origins and functional significance of these cells, including in more polyclonal systems and with other immunogens.

MATERIALS AND METHODS

Mice and immunizations. The Vh186.2 Tg, AM14 HL CB17, and B1-8 knock-in mouse strains have been previously described (25, 32, 54). (m+s)Ig and mIg Tg mice were maintained on the Jh−/− strain to ensure all B cells expressed the IgH Tg. B6 mice were purchased from The Jackson Laboratory. Mice were immunized intraperitoneally at 6–12 wk of age with either 50 μg of alum-precipitated NP$_{20}$-chicken γ globulin or alum precipitate only as the control. Hyperimmunization consisted of two doses of alum-precipitated Ag 6 wk apart. In the cell transfer system, recipients were AM14 HL CB17 mice, which were given $2–5 \times 10^6$ NP$^+$ cells from mIg Tg donors and then immunized within 18 h after transfer. All animal experiments were approved by the Yale Institutional Animal Care and Use Committee.

BrdU detection. For BrdU labeling, mice were given i.p. injections of 0.6 mg BrdU (Sigma-Aldrich) in PBS every 12 h from 11 to 14 d after immunization. Detection of BrdU in cells was essentially as previously described (26, 55).

Flow cytometry and reagents used. Single-cell suspensions of RBC-depleted splenocytes from BrdU-labeled alum or immune (m+s)Ig mice were stained with NIP-haptenated PE (NIP-PE) and FITC- or Alexa Fluor 647–labeled anti-BrdU. These were used in combination with the following Abs: Biotin-labeled CD40 (3/23), CD27 (L6.3A10), CD19 (1D3), CD38 (clone 90), IL-4Ra (mIL-4R-M1), CD22, CD35 (8C12), and CD95 (Jo-2), along with PE-labeled CD80 (16-10A) (1), Abs to CD86 (GL1), CD73, and CD23 (B3B4) were purchased from BD Biosciences; the FITC anti–Bcl-2 (3F11) kit was also purchased from BD Biosciences. PE/Cy7 streptavidin was purchased from BioLegend. Unlabeled rabbit polyclonal anti–Bcl-xL was obtained from Santa Cruz Biotechnologies. Biotin-labeled Abs to CD24 (30F1), CD44 (Pgp-1), CD11b (Mac-1), and CD62L (Mel-14), along with Alexa Fluor 488–labeled anti–I-A^d (MKD6), were purified and labeled according to the manufacturer's guidelines. Unlabeled goat anti–λ light chain (Southern Biotech) was conjugated to Alexa Fluor 405 according to the manufacturer's guidelines (Invitrogen). Biotin-labeled Abs to CD43 (S7), VLA-4, CD11a (LFA-1, M17/4), CD54 (ICAM-1), CD45RB (C363.16A), and BLA-1 were provided by T. Waldschmidt (University of Iowa, Iowa City, IA). Biotin-labeled anti-Ly6C (HK1.4) and Ly6A/E (Sca-1) were provided by A. Bothwell (Yale University, New Haven, CT). H. Kubagawa (University of Alabama, Tuscaloosa, AL) provided anti–paired immunoglobin–like receptor-A (PIR-A). Stained cell suspensions were run on a FACSAria, LSRII, or FACSCalibur (BD Biosciences).

Sorting and sequencing. For FACS sorting, spleens pooled from either immune (m+s)Ig mice (2 mice per sort, 2 sorts per time point) or immune non-Tg B6 mice (2 mice per sort, 3 sorts 13–15 wk after immunization) were treated with unlabeled anti-FcγRII/III (24.G2) and stained with Alexa Fluor 488–labeled B220 (RA3-6B2), PE-labeled CD80, and NIP-haptenated allophycocyanin (NIP-APC). Alternatively, cells were stained with FITC-labeled anti-CD35 (8C12; BD Biosciences), anti–CD80-PE, NIP-APC, and APC/Cy7-labeled anti-B220 (RA3-6B2; eBiosciences). Propidium iodide was used for live/dead discrimination. Cells were sorted on either a FACSVantage or FACSAria (BD Biosciences). Cell pellets were digested overnight at 37°C in 10 μl of digestion buffer (50 mM Tris, pH 8.0, 50 mM KCL, 0.63 mM EDTA, 0.22% NP-40, and 0.22% Tween-20) containing 0.8 μg/ml proteinase K (Novagen). Vλ1 sequences were amplified by nested PCR using Pfu Turbo polymerase (Stratagene) using external primers 5′-GCACCTCAAGTCTTG-GAGAG-3′ and 5′-ACTCTCTCTCCTGGCTCTCA-3′ and internal primers 5′-CTACACTGCAGTGGGTATGCAACAATGCG-3′ and 5′-GTTCTC-TAGACCTAGGACAGTCAGTTTGG-3′. Amplified DNA was cloned directly into pCR 4 Blunt-TOPO vector using the Zero Blunt TOPO PCR Cloning kit for sequencing (Invitrogen). Vλ1 DNA was further amplified by placing colonies directly into PCR reactions containing the primers M13 forward 5′-GTAAAACGACGGCCAG-3′ and M13 reverse 5′-CAGGAAA-CAGCTATGAC-3′. DNA was purified from the PCR reaction mixture with the QIAquick PCR Purification kit (QIAGEN), mixed with sequencing primer, T3 5′-AATTAACCCTCACTAAAGGG-3′, and sequenced by the Keck Biotechnology Resource Laboratory at Yale University School of Medicine using Applied Biosystems DNA sequencers. Sequences were aligned to a rearranged germline Vλ1/Jλ1 sequence using Lasergene DNA analysis software.

Histology. Serial sections were stained with goat anti–λ–alkaline phosphatase (AP; Southern Biotech) or the combination of FITC-labeled anti–MOMA-1 (Serotec) and biotin-labeled anti-F4/80 (C1:A3; Caltag Laboratories), using AP-conjugated anti-FITC (Invitrogen) and streptavidin (SA)-horseradish peroxidase (Vector Laboratories) as the secondary reagents, respectively. Sections were then developed with Fast Blue BB and 3-amino-9-ethyl-carbazole (Sigma-Aldrich). The sections where BrdU was to be detected were first treated with 0.07N HCl to quench any remaining AP activity, followed by fixation with a solution of 4% paraformaldehyde for 20 min. After washing with $1\times$ PBS, BrdU sections were then permeabilized with 0.1% Triton X-100 in 0.1% Na Citrate solution for 2 min on ice. Sections were treated with DNase (300 kunitz Units in 0.15 M NaCl/4.2 mM MgCl$_2$ for 30 min at room temperature) before the addition of biotin-labeled anti-BrdU (PRB-1; Phoenix Flow), followed by SA-AP (Invitrogen). BrdU staining was developed with Fast Red (Sigma-Aldrich). Using Photoshop (Adobe), brightfield images from serially stained sections were inverted to resemble immuno-fluorescent images. Channels corresponding to the appropriate marker were imported into a new Photoshop document and false colored to identify each uniquely: anti–λ was red, anti–MOMA-1 was green, and anti-F4/80 was blue. Follicular architecture, i.e., central arteriole location, was used to accurately overlay images from serial sections. BrdU$^+$/λ$^+$ cells were identified from 200× brightfield images. Areas (in arbitrary pixel units) of follicles and MZ were measured using ImagePro Plus 3.0 for a Mac.

Statistics. Simple statistical tests used are indicated adjacent to P values in the text.

Online supplemental material. Fig. S1 shows the identification of CD80$^+$ memory cells in additional mouse models. Fig. S2 shows the coexpression of CD80 and CD73 on memory cells in three different model systems. Fig. S3 shows the kinetics of GC frequency and size as determined by histology in immunized (m+s)Ig Tg mice. Fig. S4 shows CD38 expression on putative memory B cells sorted from B6 mice 15 wk after immunization, demonstrating that they are not GC B cells, which would be CD38^{lo}. The online version of this article is available at http://www.jem.org/cgi/content/full/jem.20062571/DC1.

REFERENCES

1. Ahmed, R., and D. Gray. 1996. Immunological memory and protective immunity: understanding their relation. *Science*. 272:54–60.

2. Bernasconi, N.L., E. Traggiai, and A. Lanzavecchia. 2002. Maintenance of serological memory by polyclonal activation of human memory B cells. *Science*. 298:2199–2202.

3. Dutton, R.W., L.M. Bradley, and S.L. Swain. 1998. T cell memory. *Annu. Rev. Immunol*. 16:201–223.

4. Tangye, S.G., D.T. Avery, E.K. Deenick, and P.D. Hodgkin. 2003. Intrinsic differences in the proliferation of naive and memory human B cells as a mechanism for enhanced secondary immune responses. *J. Immunol*. 170:686–694.

5. Agematsu, K., H. Nagumo, F.C. Yang, T. Nakazawa, K. Fukushima, S. Ito, K. Sugita, T. Mori, T. Kobata, C. Morimoto, and A. Komiyama. 1997. B cell subpopulations separated by CD27 and crucial collaboration of CD27+ B cells and helper T cells in immunoglobulin production. *Eur. J. Immunol*. 27:2073–2079.

6. Klein, U., K. Rajewsky, and R. Kuppers. 1998. Human immunoglobulin (Ig)M+IgD+ peripheral blood B cells expressing the CD27 cell surface antigen carry somatically mutated variable region genes: CD27 as a general marker for somatically mutated (memory) B cells. *J. Exp. Med*. 188:1679–1689.

7. Maurer, D., W. Holter, O. Majdic, G.F. Fischer, and W. Knapp. 1990. CD27 expression by a distinct subpopulation of human B lymphocytes. *Eur. J. Immunol*. 20:2679–2684.

8. Klein, U., Y. Tu, G.A. Stolovitzky, J.L. Keller, J. Haddad Jr., V. Miljkovic, G. Cattoretti, A. Califano, and R. Dalla-Favera. 2003. Transcriptional analysis of the B cell germinal center reaction. *Proc. Natl. Acad. Sci. USA*. 100:2639–2644.

9. Tangye, S.G., D.T. Avery, and P.D. Hodgkin. 2003. A division-linked mechanism for the rapid generation of Ig-secreting cells from human memory B cells. *J. Immunol*. 170:261–269.

10. Weller, S., M.C. Braun, B.K. Tan, A. Rosenwald, C. Cordier, M.E. Conley, A. Plebani, D.S. Kumararatne, D. Bonnet, O. Tournilhac, et al. 2004. Human blood IgM "memory" B cells are circulating splenic marginal zone B cells harboring a prediversified immunoglobulin repertoire. *Blood*. 104:3647–3654.

11. Smith, K.G., G.J. Nossal, and D.M. Tarlinton. 1995. Fas is highly expressed in the germinal center but is not required for regulation of the B-cell response to antigen. *Proc. Natl. Acad. Sci. USA*. 92:11628–11632.

12. Takahashi, Y., H. Ohta, and T. Takemori. 2001. Fas is required for clonal selection in germinal centers and the subsequent establishment of the memory B cell repertoire. *Immunity*. 14:181–192.

13. Liu, A.H., P.K. Jena, and L.J. Wysocki. 1996. Tracing the development of single memory-lineage B cells in a highly defined immune response. *J. Exp. Med*. 183:2053–2063.

14. Ridderstad, A., and D.M. Tarlinton. 1998. Kinetics of establishing the memory B cell population as revealed by CD38 expression. *J. Immunol*. 160:4688–4695.

15. Lalor, P.A., G.J. Nossal, R.D. Sanderson, and M.G. McHeyzer-Williams. 1992. Functional and molecular characterization of single, (4-hydroxy-3-nitrophenyl)acetyl (NP)-specific, IgG1+ B cells from antibody-secreting and memory B cell pathways in the C57BL/6 immune response to NP. *Eur. J. Immunol*. 22:3001–3011.

16. Barrington, R.A., O. Pozdnyakova, M.R. Zafari, C.D. Benjamin, and M.C. Carroll. 2002. B lymphocyte memory: role of stromal cell complement and FcγRIIB receptors. *J. Exp. Med*. 196:1189–1199.

17. Takahashi, Y., A. Inamine, S. Hashimoto, S. Haraguchi, E. Yoshioka, N. Kojima, R. Abe, and T. Takemori. 2005. Novel role of the Ras cascade in memory B cell response. *Immunity*. 23:127–138.

18. Bar-Or, A., E.M. Oliveira, D.E. Anderson, J.I. Krieger, M. Duddy, K.C. O'Connor, and D.A. Hafler. 2001. Immunological memory: contribution of memory B cells expressing costimulatory molecules in the resting state. *J. Immunol*. 167:5669–5677.

19. Liu, Y.J., C. Barthelemy, O. de Bouteiller, C. Arpin, I. Durand, and J. Bancherau. 1995. Memory B cells from human tonsils colonize mucosal epithelium and directly present antigen to T cells by rapid up-regulation of B7-1 and B7-2. *Immunity*. 2:239–248.

20. Tangye, S.G., Y.J. Liu, G. Aversa, J.H. Phillips, and J.E. de Vries. 1998. Identification of functional human splenic memory B cells by expression of CD148 and CD27. *J. Exp. Med*. 188:1691–1703.

21. Sallusto, F., D. Lenig, R. Forster, M. Lipp, and A. Lanzavecchia. 1999. Two subsets of memory T lymphocytes with distinct homing potentials and effector functions. *Nature*. 401:708–712.

22. Klein, U., R. Kuppers, and K. Rajewsky. 1997. Evidence for a large compartment of IgM-expressing memory B cells in humans. *Blood*. 89:1288–1298.

23. Bothwell, A.L.M., M. Paskind, M. Reth, T. Imanishi-Kari, K. Rajewsky, and D. Baltimore. 1981. Heavy chain variable region contribution to the NPb family of antibodies: somatic mutation evident in a γ2a variable region. *Cell*. 24:625–637.

24. Toellner, K.M., W.E. Jenkinson, D.R. Taylor, M. Khan, D.M. Sze, D.M. Sansom, C.G. Vinuesa, and I.C. MacLennan. 2002. Low-level hypermutation in T cell–independent germinal centers compared with high mutation rates associated with T cell–dependent germinal centers. *J. Exp. Med*. 195:383–389.

25. Hannum, L.G., A.M. Haberman, S.M. Anderson, and M.J. Shlomchik. 2000. Germinal center initiation, variable gene region hypermutation, and mutant B cell selection without detectable immune complexes on follicular dendritic cells. *J. Exp. Med*. 192:931–942.

26. Anderson, S.M., L.G. Hannum, and M.J. Shlomchik. 2006. Memory B cell survival and function in the absence of secreted antibody and immune complexes on follicular dendritic cells. *J. Immunol*. 176:4515–4519.

27. Dunn-Walters, D.K., P.G. Isaacson, and J. Spencer. 1995. Analysis of mutations in immunoglobulin heavy chain variable region genes of microdissected marginal zone (MGZ) B cells suggests that the MGZ of human spleen is a reservoir of memory B cells. *J. Exp. Med*. 182:559–566.

28. Liu, Y.J., S. Oldfield, and I.C. MacLennan. 1988. Memory B cells in T cell-dependent antibody responses colonize the splenic marginal zones. *Eur. J. Immunol*. 18:355–362.

29. Coico, R.F., B.S. Bhogal, and G.J. Thorbecke. 1983. Relationship of germinal centers in lymphoid tissue to immunologic memory. VI. Transfer of B cell memory with lymph node cells fractionated according to their receptors for peanut agglutinin. *J. Immunol*. 131:2254–2257.

30. Schittek, B., and K. Rajewsky. 1990. Maintenance of B-cell memory by long-lived cells generated from proliferating precursors. *Nature*. 346:749–751.

31. Obukhanych, T.V., and M.C. Nussenzweig. 2006. T-independent type II immune responses generate memory B cells. *J. Exp. Med*. 203:305–310.

32. Lam, K.-P., R. Kuhn, and K. Rajewsky. 1997. In vivo ablation of surface immunoglobulin on mature B cells by inducible gene targeting results in rapid cell death. *Cell*. 90:1073–1083.

33. Oliver, A.M., F. Martin, and J.F. Kearney. 1999. IgMhighCD21high lymphocytes enriched in the splenic marginal zone generate effector cells more rapidly than the bulk of follicular B cells. *J. Immunol*. 162:7198–7207.

34. Jacob, J., G. Kelsoe, K. Rajewsky, and U. Weiss. 1991. Intraclonal generation of antibody mutants in germinal centres. *Nature*. 354:389–392.

35. Shlomchik, M.J., A.H. Aucoin, D.S. Pisetsky, and M.G. Weigert. 1987. Structure and function of anti-DNA autoantibodies derived from a single autoimmune mouse. *Proc. Natl. Acad. Sci. USA*. 84:9150–9154.

36. Shlomchik, M.J., S. Litwin, and M. Weigert. 1990. The influence of somatic mutation on clonal expansion. *Prog. Immunol. Proc. 7th Int. Cong. Immunol*. 7:415-423.

37. Liu, Y.J., J. Zhang, P.J. Lane, E.Y. Chan, and I.C. MacLennan. 1991. Sites of specific B cell activation in primary and secondary responses

to T cell–dependent and T cell–independent antigens. *Eur. J. Immunol.* 21:2951–2962.

38. Cuss, A.K., D.T. Avery, J.L. Cannons, L.J. Yu, K.E. Nichols, P.J. Shaw, and S.G. Tangye. 2006. Expansion of functionally immature transitional B cells is associated with human-immunodeficient states characterized by impaired humoral immunity. *J. Immunol.* 176:1506–1516.

39. Kraal, G., and M. Janse. 1986. Marginal metallophilic cells of the mouse spleen identified by a monoclonal antibody. *Immunology.* 58:665–669.

40. Fuchs, E.J., and P. Matzinger. 1992. B cells turn off virgin but not memory T cells. *Science.* 258:1156–1159.

41. Ronchese, F., and B. Hausmann. 1993. B lymphocytes in vivo fail to prime naive T cells but can stimulate antigen-experienced T lymphocytes. *J. Exp. Med.* 177:679–690.

42. Rothstein, T.L. 2000. Inducible resistance to Fas-mediated apoptosis in B cells. *Cell Res.* 10:245–266.

43. Zhang, N., D. Yang, H. Dong, Q. Chen, D.I. Dimitrova, T.J. Rogers, M. Sitkovsky, and J.J. Oppenheim. 2006. Adenosine A2a receptors induce heterologous desensitization of chemokine receptors. *Blood.* 108:38–44.

44. Yamashita, Y., S.W. Hooker, H. Jiang, A.B. Laurent, R. Resta, K. Khare, A. Coe, P.W. Kincade, and L.F. Thompson. 1998. CD73 expression and fyn-dependent signaling on murine lymphocytes. *Eur. J. Immunol.* 28:2981–2990.

45. Weninger, W., M.A. Crowley, N. Manjunath, and U.H. von Andrian. 2001. Migratory properties of naive, effector, and memory CD8⁺ T cells. *J. Exp. Med.* 194:953–966.

46. MacLennan, I.C., M. Casamayor-Palleja, K.M. Toellner, A. Gulbranson-Judge, and J. Gordon. 1997. Memory B-cell clones and the diversity of their members. *Semin. Immunol.* 9:229–234.

47. Good, K.L., V.L. Bryant, and S.G. Tangye. 2006. Kinetics of human B cell behavior and amplification of proliferative responses following stimulation with IL-21. *J. Immunol.* 177:5236–5247.

48. Toyama, H., S. Okada, M. Hatano, Y. Takahashi, N. Takeda, H. Ichii, T. Takemori, Y. Kuroda, and T. Tokuhisa. 2002. Memory B cells without somatic hypermutation are generated from Bcl6-deficient B cells. *Immunity.* 17:329–339.

49. Weller, S., A. Faili, C. Garcia, M.C. Braun, F.F. Le Deist, G.G. de Saint Basile, O. Hermine, A. Fischer, C. Reynaud, and J. Weill. 2001. CD40-CD40L independent Ig gene hypermutation suggests a second B cell diversification pathway in humans. *Proc. Natl. Acad. Sci. USA.* 98:1166–1170.

50. Chappell, C.P., and J. Jacob. 2006. Identification of memory B cells using a novel transgenic mouse model. *J. Immunol.* 176:4706–4715.

51. Alugupalli, K.R., J.M. Leong, R.T. Woodland, M. Muramatsu, T. Honjo, and R.M. Gerstein. 2004. B1b lymphocytes confer T cell-independent long-lasting immunity. *Immunity.* 21:379–390.

52. Hsu, M.C., K.M. Toellner, C.G. Vinuesa, and I.C. Maclennan. 2006. B cell clones that sustain long-term plasmablast growth in T-independent extrafollicular antibody responses. *Proc. Natl. Acad. Sci. USA.* 103:5905–5910.

53. Kraus, M., M.B. Alimzhanov, N. Rajewsky, and K. Rajewsky. 2004. Survival of resting mature B lymphocytes depends on BCR signaling via the Igalpha/beta heterodimer. *Cell.* 117:787–800.

54. Shlomchik, M.J., D. Zharhary, T. Saunders, S. Camper, and M. Weigert. 1993. A rheumatoid factor transgenic mouse model of autoantibody regulation. *Int. Immunol.* 5:1329–1341.

55. Allman, D.M., S.E. Ferguson, V.M. Lentz, and M.P. Cancro. 1993. Peripheral B cell maturation. II. Heat-stable antigen(hi) splenic B cells are an immature developmental intermediate in the production of long-lived marrow-derived B cells. *J. Immunol.* 151:4431–4444.